



Article

A Remote Sensing-Based Inventory of West Africa Tropical Forest Patches: A Basis for Enhancing Their Conservation and Sustainable Use

Vladimir R. Wingate ^{*}, Felicia O. Akinyemi, Chima J. Iheaturu and Chinwe Ifejika Speranza

Land Systems and Sustainable Land Management, Institute of Geography, University of Bern, Hallerstrasse 12, 3012 Bern, Switzerland

* Correspondence: vladimir.wingate@giub.unibe.ch

Abstract: The rate of tropical deforestation is increasing globally, and the fragmentation of remaining forests is particularly high in arable landscapes of West Africa. As such, there is an urgent need to map and monitor these remnant forest patches/fragments and so identify their multiple benefits and values. Indeed, recognizing their existence will help ensure their continued provision of ecosystem services while facilitating their conservation and sustainable use. The aim of this study is therefore to inventory and characterise the current extent and change of remnant forest patches of West Africa, using multi-source remote sensing products, time-series analyses, and ancillary datasets. Specifically, we collate and analyse descriptive and change metrics to provide estimates of fragment size, age, biophysical conditions, and relation to social-ecological change drivers, which together provide novel insights into forest fragment change dynamics for over four decades. We map forest patches outside protected areas with a tree cover $\geq 30\%$, a tree height of ≥ 5 m, an area ≥ 1 km² and ≤ 10 km². Appended to each patch are descriptive and change dynamics attributes. We find that most fragments are small, secondary forest patches and these cumulatively underwent the most forest loss. However, on average, larger patches experience more loss than smaller ones, suggesting that small patches persist in the landscape. Primary forest patches are scarce and underwent fewer losses, as they may be less accessible. In 1975 most patches were mapped as secondary, degraded forests, savanna, woodland, and mangrove, and relatively few comprised cropland, settlements, and agriculture, suggesting that new forest patches rarely emerged from arable land over the past 45 years (1975–2020), but rather are remnants of previously forested landscapes. Greening is widespread in larger secondary fragments possibly due to regrowth from land abandonment and migration to urban areas. Forest loss and gain are greater across fragments lying in more modified landscapes of secondary forests, while forest loss increases with distance to roads. Finally, larger forest patches harbour a denser tree cover and higher trees as they may be less impacted by human pressures. The number and extent of West African forest patches are expected to further decline, with a concurrent heightening of forest fragmentation and accompanying edge effects. Lacking any conservation status, and subject to increasing extractive demands, their protection and sustainable use is imperative.

Keywords: remote sensing; forest fragmentation; forest patches; forest change; forest inventory



Citation: Wingate, V.R.; Akinyemi, F.O.; Iheaturu, C.J.; Ifejika Speranza, C. A Remote Sensing-Based Inventory of West Africa Tropical Forest Patches: A Basis for Enhancing Their Conservation and Sustainable Use. *Remote Sens.* **2022**, *14*, 6251. <https://doi.org/10.3390/rs14246251>

Academic Editor: Xiangzheng Deng

Received: 28 September 2022

Accepted: 6 December 2022

Published: 9 December 2022

Publisher's Note: MDPI stays neutral with regard to jurisdictional claims in published maps and institutional affiliations.



Copyright: © 2022 by the authors. Licensee MDPI, Basel, Switzerland. This article is an open access article distributed under the terms and conditions of the Creative Commons Attribution (CC BY) license (<https://creativecommons.org/licenses/by/4.0/>).

1. Introduction

Tropical forests are a crucial component of the earth system, providing ecosystem services ranging from biodiversity conservation to climate regulation [1,2]. Concurrently, anthropogenic land cover and land-use change are driving increasing rates of tropical deforestation and fragmentation, jeopardizing the continued provisioning of their services and functions [3–10]. Commodity demands on the international market and consequent conversion of forested lands to agricultural land-uses chiefly drive this process. In addition,

the extension of urban settlements and other human land-uses such as infrastructure, small-scale clearing, selective logging, management by fire, and the synergies and feedbacks between these, are major drivers of tropical forest loss and fragmentation [11–13]. Despite the growing evidence that tropical forests are essential for ecosystem functions and services, as well as social well-being, forest loss and fragmentation from human pressures continue unabated and at an increasing rate [12].

Tropical forests fragmentation negatively impacts forest functioning; for instance, the greater forest edge leads to increased drying, risk of fire, and a concurrent loss of biodiversity and carbon storage [8,10,14,15]. Moreover, the remaining smaller fragments are disproportionately impacted by these effects, and this is often compounded by more intense anthropogenic exploitation [5,16,17]. In particular, the length of forest edge has dramatically increased, with the greatest rise found on the African continent [18].

Global forest change datasets have enabled unprecedented ability to monitoring global changes in forest cover; concurrently, wall-to-wall forest fragmentation analyses have provided invaluable insights into the scale and impact of the process [18,19]. For instance, Hansen et al. (2020) identify all tropical forest fragments from 10–1,000,000 km² [20]. Yet, the smaller forest fragments (≤ 10 km²) of West Africa, which are the focus of this study, have received less attention. Further, little evidence exists to show whether and why forests are persisting, resurging, or emerging, and what factors are driving the process [21]. For example, in Latin America, tropical forest recovery has been linked to complex interactions of globalization-based processes such as remittances, national agrarian- and land reforms, new environmental ideologies, and local land management practices [21]. A prominent narrative is that forest loss and fragmentation are driven by timber extraction and subsequent conversion to agricultural land-use, leaving forest remnants; yet West African forest fragments or patches (terms used interchangeably) are also known to be created and conserved by land users [22].

To identify whether forest patches are remnants or the result of sustainable management and conservation practices or associated processes, it is first necessary to map them, estimate their age, and identify whether they comprise primary or secondary forest. There is a corollary need to inventory and characterise them, assess how they are changing and to what pressures they are subject to, and so help further value their multiple functions and benefits. Such information also provides the basis for in-depth social-ecological analyses, aimed at informing measures to reduce human pressures and fostering conservation and sustainable use. Importantly, a comprehensive knowledge of West African forest patch characteristics, spatial-temporal dynamics, and their social-ecological contexts, is prerequisite to ensure their conservation and sustainable use. However, this information is either non-existent or has yet to be collated; and further, an understanding of the rate and extent of changes occurring in forest patches, and whether they persist in the landscape it still lacking.

The aims of this study are therefore twofold; firstly, to develop a regional West African forest patch inventory using remote sensing products and ancillary data; and secondly, to quantify the change dynamics experienced by forest patches across size classes, and thereby identify regional ecological changes to help target management and conservation actions.

To address these aims, our specific objectives are to (i) map and inventory forest fragments using an approach based on existing remote sensing products, cloud computing and object-based analyses, (ii) append to each fragment descriptive biophysical metrics, social-ecological indicators, and multi-temporal land-use and landcover data, thereby enabling forest patch change dynamics to be characterised, (iii) examine the relationships between patch size class and biophysical metrics and indicators, and finally, (iv) map past land-use and land cover of fragments. Thus, here we present a method to map forest fragments, together with a map-based inventory, a description of their characteristics, and an appraisal of how they are changing across size classes.

2. Methodology

2.1. Study Area

The study region encompasses the countries of Togo, Benin, Nigeria, and Cameroon (Figure 1). In these countries, rising competition for land, low agricultural productivity, limited access to knowledge and technology drives many smallholders to clear forests for agriculture in a pattern of shifting cultivation [23–25]. Further, deforestation is driven by unsustainable logging practices, fuel wood collection and commercial agriculture [26]. Indeed, over 51% of West Africa’s population (200 million people) depend on agriculture for their livelihoods, thereby heightening the threats of deforestation and land degradation [27].

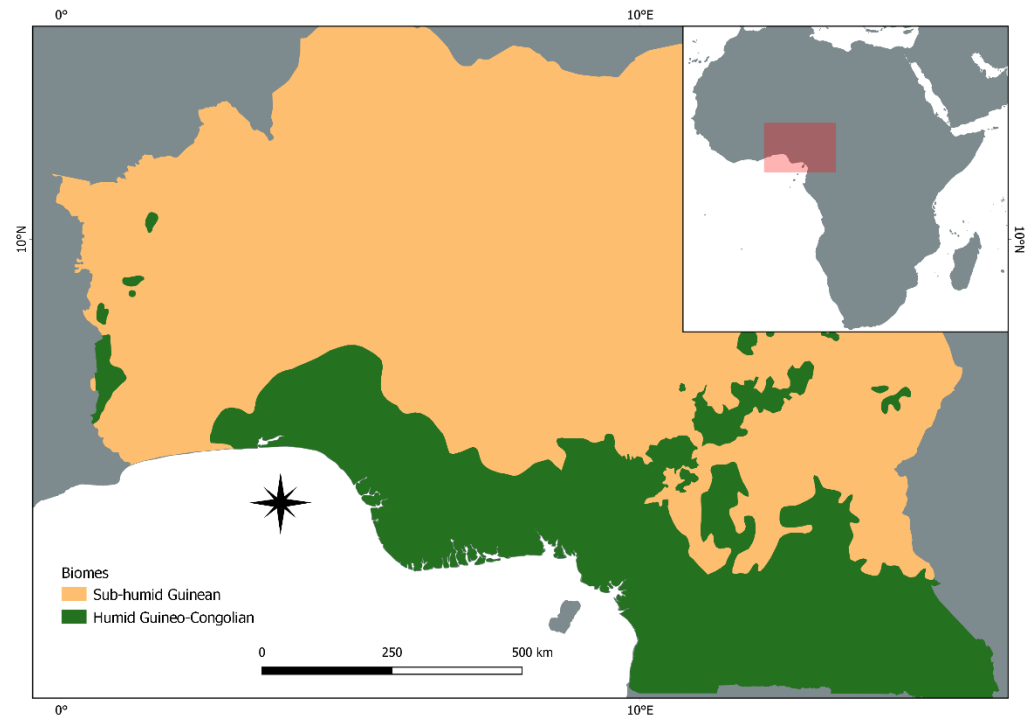


Figure 1. Study region encompassing the countries of Togo, Benin, Nigeria, and Cameroon, with in the Guinean and humid Guineo-Congolian biomes.

The study region encompasses the two distinct biomes, namely, the sub-humid Guinean and humid Guineo-Congolian. Soils vary widely across the region but are mainly deep lateritic. In the Sudan zone maize, groundnuts, and cowpeas are grown; root crops such as cassava and yams are found mostly across the Guinean zone, while tree crops such as cocoa, palm trees, or cashew trees in addition to root crops, are found in the Guineo-Congolian zone [28].

Rainfall across West Africa has a south to north decreasing gradient. Vegetation distribution matches the mean annual rainfall distribution ranging from the Guineo-Congolian zone in the south (2200–5000 mm), and northwards, the sub-humid Guinea savanna (1000–1500 mm), the dry sub-humid Sudan savanna (600–1000 mm) [28,29]. Most of West Africa has one rainy season, which lasts from one to six months; the area with two rainy seasons (a long and short one), is restricted to the southern parts of the coastal countries from Togo to Cameroon and is related to the advance and retreat of the intertropical convergence zone. In the dry season, an anticyclonic high pressure centered over the Sahara drives the Harmattan (December–March), a dry wind from the northeast, while during the rainy season, a depression brings warm, moist air from the Gulf of Guinea. In the Sudan zone, vegetation comprises open tree savannas to wooded savannas to open woodlands with tall, perennial grasses. In the north, tree savannas dominate, while in south, denser wooded savannas and open woodlands are frequent. Fire characterises the region’s ecology, with natural and human-made fires burning up to 80 percent of the region annually.

Gallery forests harbouring tall tree species frequent in the Guinean Region grow along watercourses, at times reaching far into the north; they are rarely affected by bush fires and act as natural fire breaks [28].

The Guinea savanna, which extends across most of the study area, is also one of the most critically fragmented regions, with only 68,500 km², or 10 percent of its former forest extent remaining. Indeed, much of the forests are heavily exploited for timber and hunting. Seasonally wet-and-dry deciduous or semideciduous forest predominate; high rainfall and a pronounced dry season lasting between 7 to 8 months distinguishes it from the southern Guineo-Congolian and northern Sudanian regions. The forest canopy is dense and closed, generally not affected by fires, creating a varied woody understory, with tree heights averaging 18 to 20 m. The present-day forests and arable landscapes of the region are heavily impacted by human activity, in particular slash-and burn agriculture but also urbanization; the result is that the actual remaining extent of Guinean forests is quite limited, and this is markedly altered. Wooded savanna forms an extensive component of the region, although gallery forests of varying width length are frequently found along watercourses [30]. Some authors propose that the forests have mostly been replaced by secondary savanna (derived savanna), consisting of arable mosaics, fallow and secondary bush and forest, and caused by long-term (centuries) human influence [31–36].

Derived savanna, converted through human use from forests occur between the Guinea savanna and the Guineo-Congolian zones and are sometimes subsumed under the Guinea Savanna [28,37]. The remainder of study site straddles the Guineo-Congolian Region; rainfall is either distributed across the year or occurs in two rainy seasons with brief dry periods. The region is divided geographically into western and eastern parts by the Dahomey Gap, a broad branch of the Guinean region reaching the coast. Today, only a fraction of the land remains forested, yet the forest flora is the most biodiverse in West Africa, with dense forests and trees of over 60 m, the upper tier usually being a discontinuous canopy high over a dense lower canopy. Woody climbers and epiphytes are characteristic in the undergrowth, and herbaceous cover may also be present [28].

Over 50 years of satellite imagery have demonstrated that contiguous blocks of forest across much of the Sudanian, Guinean and Guineo-Congolian regions have been greatly diminished by land conversion; yet a myriad of small forest islands or patches have persisted across time and are spread out in savannas across the region. Often, they have a village either adjacent or at their centre. Evidence is emerging that for the past century experts have misinterpreted these landscapes, falsely concluding that these forested islands were remnants of a continuous dense forest that once blanketed the region [22]. The idea of widespread deforestation predominated during the colonial period and is still widely held—yet accounts from colonial reports speak of savanna landscapes rather than forest. Further, reports of village elders suggest that some forest islands are not remnants of deforestation, but rather forests established by previous generations in a savanna landscape [22]. Available aerial imagery from 1952 confirms this hypothesis and provides ample evidence of a savanna landscape with dispersed forest patches, such as it appeared in the 1990s [22]. This phenomenon is presumably more pronounced in the less wooded Sudanian and Guinean regions, but less so for the Guineo-Congolian region. Analysis of historical imagery further reveals the fragments are remarkably stable over time, and often associated with a village. Such patches are found across all the southern countries of West Africa; of these, Benin is remarkable for its roughly 3000 sacred forests [38]. Such patches are sacred when they conserve a sacred spring or site, although they can also be places of ritual significance and initiation. They are not always restricted to the local population, although permission is often required for extracting forest products such as game, timber, firewood, medicinal plants, and fruits [38]. In this study, we map all remaining forest fragments across four countries and spanning three major and highly distinct biomes, to provide a basis for informing their conservation and sustainable use.

2.2. Forest Patch Detection

We developed a forest patch detection workflow and implemented it in Google Earth Engine [39] (Figure 2). The Hansen et al. (2013) tree cover dataset for the year 2000 was used to identify forest patches across the tropical humid forest biomes of West Africa, as it provides a medium spatial resolution (30 m) data, entirely encompassing the study area, while being the most established forest change detection dataset available [19]. It must be noted this dataset does not distinguish between natural and plantation forests; rather, it provides a continuous estimate of percentage tree cover.

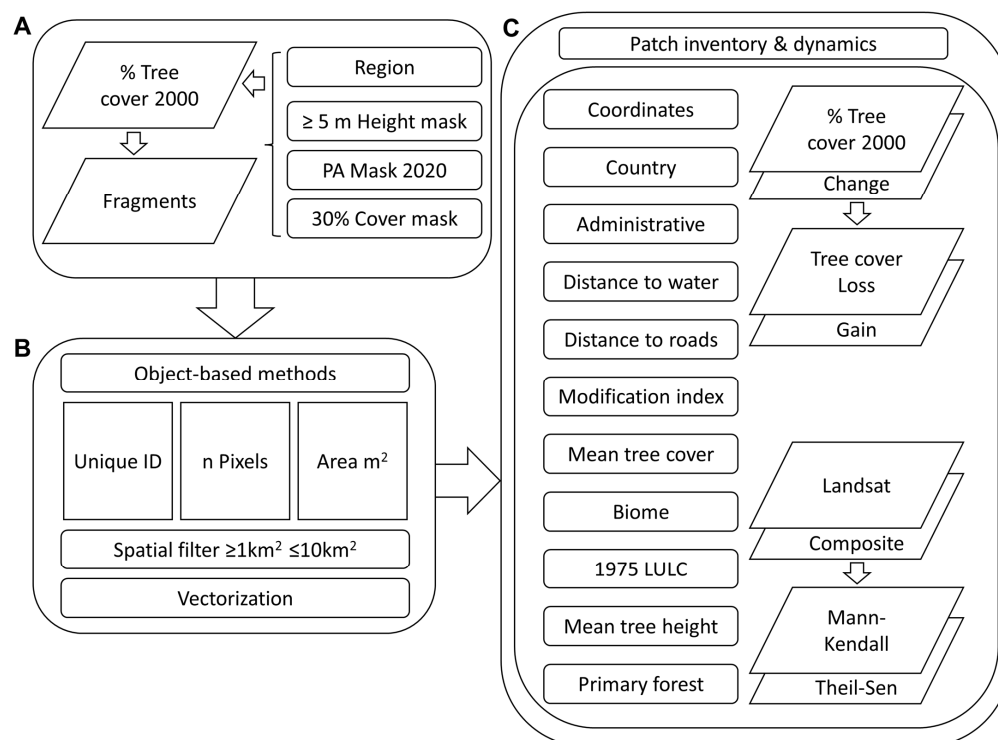


Figure 2. Workflow detailing the forest patch detection approach. (A) A threshold of 30% tree cover, tree height mask of ≥ 5 m, a protected area mask and a country filter. The resulting forest fragments are processed using object-based methods (B), inventory attributes are appended to the resulting forest patches (C).

We used a modified definition to that of the Food and Agricultural Organization (FAO), which defines forest as land ≥ 0.5 ha with trees taller ≥ 5 m and a canopy cover $\geq 10\%$. Specifically, in this study, forest patches are defined as having a tree cover $\geq 30\%$, a tree height of ≥ 5 m, and an area ≥ 1 km²– ≤ 10 km². We exclude forests ≥ 10 km² as they are likely not embedded in agricultural landscapes and have been analysed elsewhere in the literature [18–20,40]. Similarly, we exclude patches ≤ 1 km² as the resulting number of fragments would be too large to effectively validate (i.e., confirm by independent observation), and moreover, the resulting fragments are not readily distinguishable from the surrounding landscape as forest fragments based on available ancillary datasets. A canopy cover $\geq 30\%$ was chosen as this is the value used in studies such as [41], hence making our results comparable. Finally, we apply a 5 m tree height mask using the most recent high-resolution Global Ecosystem Dynamics Investigation (GED) dataset which represents global tree heights based on a fusion of spaceborne-lidar data [41]. To exclude protected areas from the analysis we use a World Database on Protected Areas (WDPA) mask [42]. To generate a map of forest patches in the year 2021, a threshold of 30% tree cover is applied to the year 2000 tree cover dataset, and all changes (tree cover loss and gain) are masked out, resulting in a current map of forest patches with a tree cover $\geq 30\%$ [19]. An object-based algorithm then assigned each forest patch a unique identifier number; the area

of each object was computed using pixel resolution and number of pixels per object, and objects were then filtered by their area, with patches $\leq 1 \text{ km}^2$ and $\geq 10 \text{ km}^2$ being omitted. The raster dataset was resampled to a spatial resolution of 90 m and converted to vector format to append information to its attribute table. Figure 1 shows a workflow detailing the approach and inventory variables.

2.3. Inventory Attributes

Variables listed in Table 1 are appended to each patch. Since patches harbouring primary forests harbour more biodiversity and provide greater climate benefit [41,43], we used the primary forest mask of [44], which defines primary forests as “tall, dense tree cover absent of observable disturbance in the satellite record”. We classified all patches containing a fraction of primary forest as primary forest and consider all forests patches which are not found in primary forest to be secondary forests and assume these forests to be older than 20 years, since they already had the attributes of a forest, namely tree $\geq 5 \text{ m}$ high, and tree cover ≥ 30 percent in the year 2000. To identify past land-use/land cover we leverage the USGS West Africa 1975 map [28]. In this way, we can estimate the age of the forest patch, i.e., < 45 years (1975–2000) or > 45 years (1975–2020); however, this dataset is not available for Cameroon and as such we omit this country from our analysis. Latitude and longitude were computed from the patch centroid, and the biome in which the patch lies was identified using the RESOLVE Ecoregions dataset (2017) [45]. Country and administrative boundaries were appended using the Global Administrative Unit Layers [46]. As hydrological connectivity and distance are important for forest composition and tree species richness [47], Euclidean distance in meters was used to measure proximity to watercourses derived from the Joint Research Centre of the European Commission Yearly Water Classification History, v1.3. This dataset maps the geographic location and temporal distribution of surface water (1984–2020), and a mask of permanent and seasonal water for the period 2000–2020 was used to assess the distance of each forest patch to water [48]. Euclidean distance in meters was used to measure the distance to roads derived from Global Roads Open Access Data Set, Version 1 [49]. The global Human Modification dataset (gHM) provides a cumulative measure of human modification of terrestrial lands globally at 1 square-kilometer resolution and may indicate the need for improved spatial planning and conservation. Values range from 0.0–1.0 are calculated by estimating the proportion of a given location that is modified, where 0 is not modified and 1 is very modified [50,51]. Tree cover loss/gain were extracted from the Hansen Global Forest Change v1.8 (2000–2020) tree cover dataset [19]. Percentage tree canopy cover for the year 2000 is defined as “canopy closure for all vegetation taller than 5 m in height”, loss as “forest loss during the study period (2000–2020) and gain as “a non-forest to forest change entirely within the study period” 2000–2012 [19]. Trend statistics include the Mann–Kendall trend test for the presence of an increasing or decreasing trend, and the Theil–Sen slope to quantify the magnitude of the trend, and thus assess whether canopy greenness of individual forest patches is increasing or decreasing. These tests were applied to a Landsat 5, 7 and 8 Normalized Difference Vegetation Index (NDVI) harmonized time-series, from which growing season maximum NDVI images were created by temporal compositing [52–57].

2.4. Analyses

Descriptive change statistics and regression models characterising the forest patches and their spatial and temporal dynamics are presented in the Results section. Regression models are used to test for a relationship between a dependent (target) and independent variable(s) (predictor) and are provided with the coefficient of determination R^2 statistic, P-Value, confidence interval and intercept. To process the regression analysis, we aggregated forest fragments into size classes to reduce the amount of noise in the analysis. Specifically, we aggregated the fragments into 1 km^2 size classes, such that if a patch were 1.5 km^2 it would be grouped into size class 1–2; this resulted in individual forest patches being aggregated into 9, 1 km^2 area/size classes of 1–2 to 9–10 km^2 comprising the predictor

variables. Subsequently, the average value of the variable of interest was taken for each forest fragment size class and comprised the target variable. For example, this results in mean tree height for across all forest fragments with an area ranging from 1–2 km², and so forth. These were graphed as a regression model, with area/size class on the X-axis and mean variable value on the Y-axis. Finally, a regression model was also processed for secondary forest patches, and patches containing fractions of primary forest, as these two forest types are expected to present distinct characteristics.

Table 1. Variables selected to inventory forest patches.

	Variable Code	Description	Date	Units
1	Labels	ID	-	-
2	Biome	Biome	-	-
3	Country	Country	-	-
4	Admin	Sub-national administrative region	-	-
5	Region	West Africa	-	-
6	D_water	Euclidian distance to water	1984–2020	Meters
7	D_roads	Euclidian distance to roads	1980–2010	Meters
8	Lat_DD	Latitude	-	Decimal degrees
9	Long_DD	Longitude	-	Decimal degrees
10	Area_m	Area of forest patch	2020	m ²
11	gHM	Global Human Modification dataset	2016	0–1
12	treeheight	Mean tree height	2019	Meters
13	treecover	Mean percentage tree-cover	2000	%
14	mask	Tree-cover binary mask	2000	Binary
15	Primary	Primary/non-primary	2001–2002	Binary
16	Gain_area	Tree cover gain area (m ²)	2000–2012	m ²
17	Loss_area	Tree cover loss area (m ²)	2000–2020	m ²
18	MannKendal	Mann–Kendall trend test	2000–2020	–1/+1
19	TheilSen	Theil-Sen slope	2000–2020	0–1

2.5. Validation

We validate the forest patch dataset using the error matrix approach [58], and focus only a single country (Nigeria) given analysts knowledge of the area, available ancillary datasets and the similarity with conditions in the other three countries (Figure 3). A proportional sampling strategy was adopted, whereby the mapped area was first divided into a systematic grid of quadrants (each measuring 295 km by 548 km). The predicted forest patches in quadrants 1, 2, 3, and 4 were 1114, 521, 163, and 260 in number, respectively. The systematic division ensured that a representative sample size was selected in each quadrant. Next, 20% of the forest patches within each quadrant was randomly selected. The choice of 20% was recommended in Congalton and Green (2019) as a proportional sample size for thematic maps [58]. The resulting sample points were 220, 95, 35, and 52 for quadrants 1, 2, 3, and 4, respectively. These points (402) were visually evaluated using Google Earth imagery by an independent analyst. Each point was classified as either a forest patch or a non-forest patch. The resulting dataset of reference points was then compared with the classified point using an error matrix.

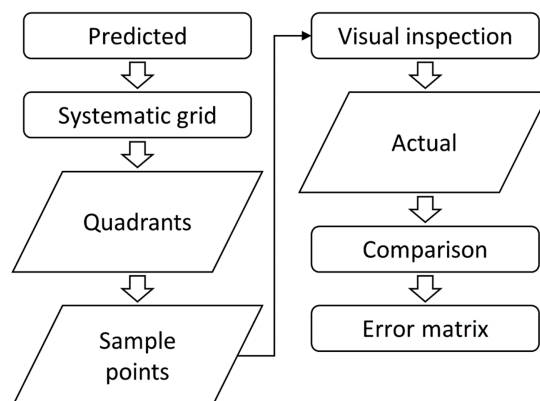


Figure 3. Workflow illustrating the forest patch validation approach.

The validation revealed 93.8% overall classification accuracy (Table 2) indicating that forest patches were effectively mapped [58].

Table 2. Validation error matrix.

Predicted	Actual		Σ User	Users' Accuracy (%)
	Forest Patch	Other		
Forest Patch	377	25	402	93.8
Other	25	377	402	93.8
Σ Producer	402	402	804	
Producers' accuracy (%)	93.8	93.8		
			Overall accuracy (%)	93.8%

3. Results and Discussion

This study inventoried 3924 forest patches fitting our proposed definition, with an area of over 9770 km² throughout the study period and across four West African countries, a region spanning 1,551,244 km², and thereby provides a basis for informing their conservation and sustainable use. Additionally, it presents a novel method to inventory tropical forest fragments based on multi-source, satellite remote sensing products. We find a cumulative forest loss estimate of 363 km² between 2000 and 2020 and gain of only 13 km² from 2000 to 2012, across all patches. Figure 4 illustrates four forest patches converted to a shapefile and overlaid on a fine spatial resolution (4.77 m) Planet base maps for the period January 2022 [59].

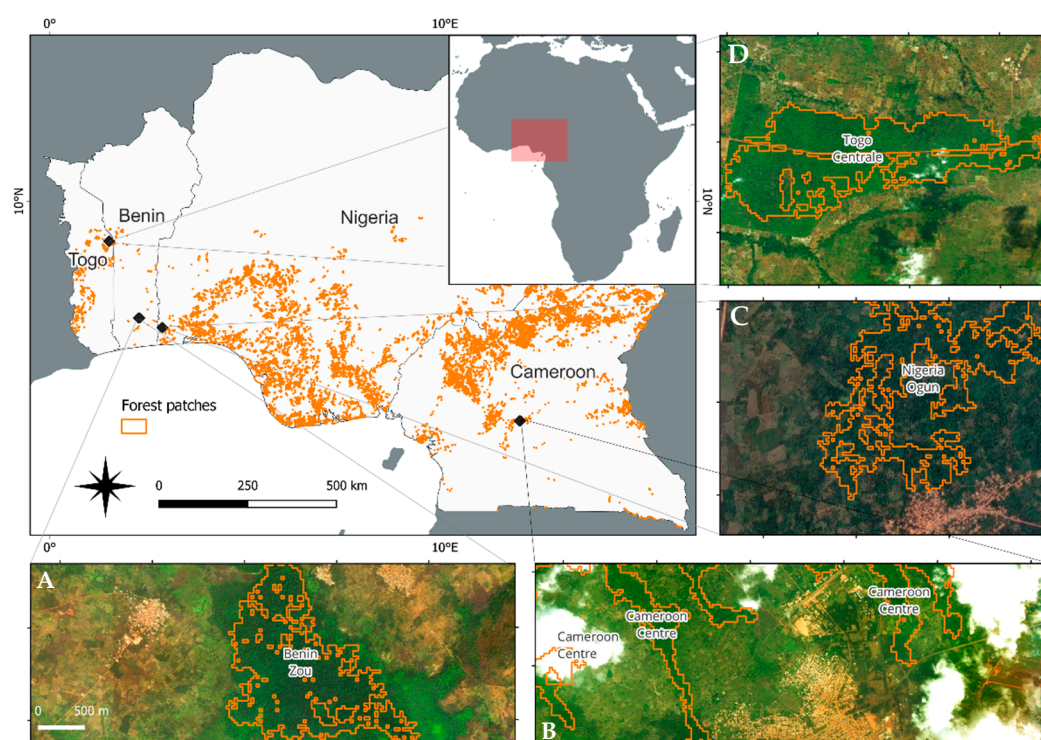


Figure 4. Figures showing forest patches samples; polygons outlined in orange are forest patches identified as fitting our proposed definition. Panel (A) sample near a village in southern Benin. Panel (B) sample near an urban and intensive agricultural area in central Cameroon. Panel (C) sample close to a highway and rural village in south-western Nigeria. Panel (D) sample in a smallholder arable mosaic in north-eastern Togo.

3.1. Change Statistics

Forest patches mapped in this study cover a vast and diverse region of West Africa, comprising different bio-climatic regions, elevations, geology and soils, land-uses, and human pressures [28]. Thus, we offer only generalized conclusions, that lay the foundation for

future in-depth studies of individual forest patches, captured in the inventory. Importantly, considering the limitation and uncertainties of the data used in the following analyses, we emphasize that our results are in fact estimates.

Figure 5A presents a bar graph of the estimated area of forest patches as a percentage of total number of patches per size class (area/sum [area]) (km²). Change, comprising tree cover loss and gain, is also shown as a percentage. Here, we estimate that almost 20% of all mapped secondary patches are found to be between 1–2 km². Concurrently, the most important tree cover loss area, as a percentage of the total number of patches, is found in the smallest size class, of secondary forests. Similarly, most tree cover loss has occurred in secondary forests, with a lower percentage taking place in primary forests across size classes. Most of the mapped forest patches are small, secondary forest patches, and these small patches are found to experience the greatest overall loss. This result is in line with previous studies showing that smaller forest fragments experience the greatest degree of forest loss [20]. Interestingly, we find that primary forest patches experience overall less change; this may be because they are more remote, less accessible, and not as widespread [60].

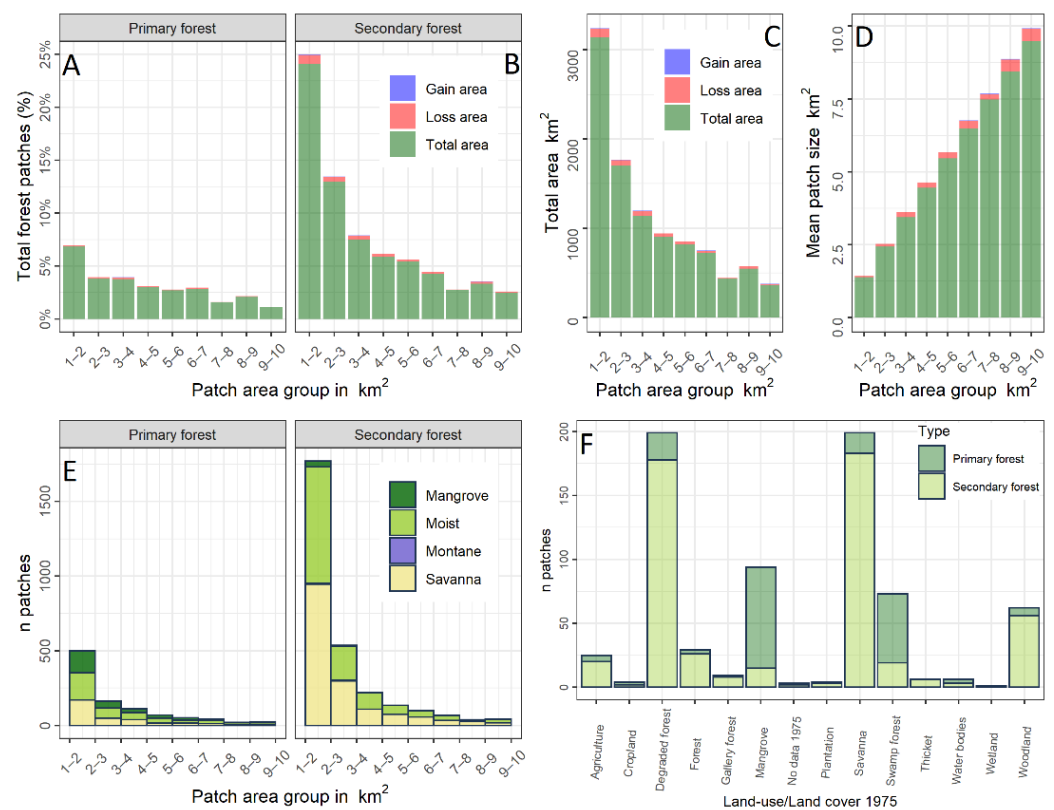


Figure 5. (A) Bar graph showing the area of forest patches as a percentage of total number of patches per size class (area/sum [area]) (km²) and whether comprising primary or (B) secondary forest; percentage change (loss and gain) is also shown. (C) The total area, area of loss, and area of gain, in each size class are graphed, revealing that most patches are small and cumulatively have lost the most area. (D) The average area of the forest patches per size class, and the average area of the loss and gain per size class; on average, large patches experience greater areal loss. (E) Frequency distribution histogram showing the number of patches across four different biomes, and whether they comprise primary or secondary forest. (F) Bar plots show the number of forest patches, their land-use/land cover in 1975, and whether they comprise primary or secondary forest.

In Figure 5B, a frequency distribution histogram shows the number of forest patches (count) grouped by size class; this plot is divided into how many forest patches are primary or contain a fraction of primary forest, or secondary forests, and illustrates in which biome

these patches are found. Further, 2931 of the 3924 mapped forest patches comprised secondary forests, ranging from savanna to woodland and degraded forest in 1975, with only 993 being mapped as primary forests. In addition, forest patches in primary forests are most often mangrove and moist broad leaf forests, while patches in secondary forests are most often moist broad leaf followed by savanna, as identified by Fischer et al. (2021) [18].

Secondary forests thus comprise the bulk of the inventoried forest patches, with those harbouring primary forests being scarce. Mangroves are important contributors to primary forest patches; indeed, these forests are extensively subject to fragmentation globally [61]. Moist forests are the second most important contributors; these results serve to highlight the conservation importance of these biomes. In contrast, secondary forests comprise moist forests and savanna. Thus, the number and size of patch per biome (Figure 5B) reflect the distribution of mapped forest patches, with the bulk of fragments found in the moist biome, followed by savanna and mangroves. Moist forests are also more likely to have dense canopy and tall canopy height, and therefore are more likely to fit the parameters defined in this study of forest cover [40].

In Figure 5C, the area, area of loss, and area of gain, of the total number of patches in each size class, are graphed. Here, the cumulative (sum) area of forest patches, and the total area of forest loss, is greatest for the patch of the smallest size class (1–2 km²). In contrast, when comparing the estimated average area, area of loss, and area of gain, of the forest patches in each size classes, we find that, on average, the larger patches had a greater average loss area, than the small patches (Figure 5D).

We expected small forest patches would undergo greater forest loss, compared to larger patches [5,17]. This we found, with the cumulative area of patches mapped being greatest for the smallest size class (1.2 km²), with over 1500 patches. Similarly, the cumulative area of forest loss is greatest for this size class, and diminishes with increasing patch size, while the cumulative area of forest gain is negligible (Figure 5C). However, when looking at change in terms of average patch size, the largest change was found for the largest patches (Figure 5D). Finally, a frequency distribution histogram showing the number of patches per size class across four different biomes, and whether they comprise primary or secondary forest, reveals that most forest patches are identified as secondary forests, although a sizeable proportion are identified as being in proximity or comprising primary forests (Figure 5E).

Land-Use/Land Cover 1975

The age of a forest is an important attribute of forest resilience [62]. Hence, information describing forest age is an important indicator for biodiversity conservation and sustainable use. Figure 5F presents a bar graph with the number of forest patches, their land-use/land cover (LULC) in 1975, and whether they comprise primary or secondary forest, thus giving us an estimate of the time that forest patch has been forested, and where new forest patches have been established on land previously used for agriculture or settlement. Omitted are forest patches with no land-use land cover mapped in 1975—these comprise patches found in Cameroon for which no such dataset exists for 1975. We find that most forest patches were mapped as forested land covers (i.e., savanna, woodland, degraded forest, forest, etc.) in 1975, and only relatively few were mapped as being either settlement (4), agriculture (78), cropland (16), settlement (4), or plantation (10) in 1975; of these, most were mapped as being secondary forests. Thus, most forest patches originated as remnants of natural vegetation during the 45-year period assessed and are classed as being older than 45 years (>45), while those which comprised human land-uses are classed as being less than 45 years (<45). For instance, we find that many secondary forest patches (601) comprised degraded forest in 1975, a comparable number were savanna (594), and fewer were woodland (210). These results suggest that most forest patches in the study area have not newly emerged or transitioned from the arable landscape since 1975, but rather, are remnants of forested landscapes (savanna, woodland, degraded forest, forest, etc.) which were present prior to 1975.

3.2. Regression Analyses

3.2.1. Forest Loss and Gain

We estimate how areal forest loss and gain vary between forest patch size classes and distinguish between those harbouring primary forests and those comprising secondary forests. In so doing we test the hypothesis that forest patch size is correlated with the amount of forest loss, with larger patches in secondary forests undergoing greater forest losses. We find a significant negative coefficient of determination ($R^2 = 0.83$, $p < 0.01$) between the average area of forest loss and patch size class in patches harbouring primary forests (i.e., smaller patches experience on average less forest loss than larger ones). This relationship is less pronounced in secondary forest patches ($R^2 = 0.74$, $p < 0.01$), however these experience larger overall losses (as secondary forests cover more total area), demonstrating that larger patches experience greater levels of forest loss (Figure 6A,B). These results may suggest that small patches persist in the landscape, while large ones experienced more overall change.

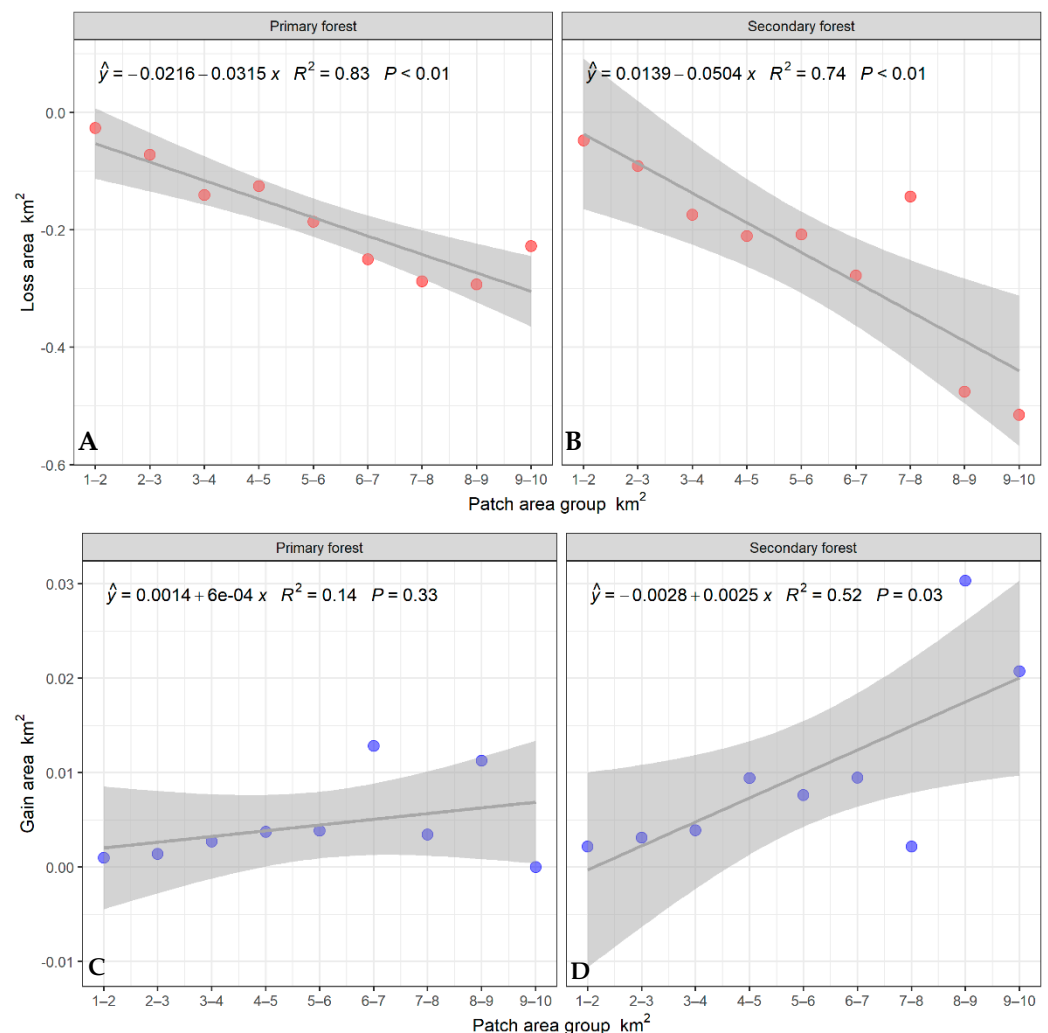


Figure 6. (A) Forest loss is more strongly related to patch size in primary forests (B) and is similarly related in secondary forests, which experience larger overall losses. (C) Similarly, forest gain is weakly related to size class in primary forest (D), yet strongly positively related to fragment size in secondary forests.

Similarly, a weak positive coefficient of determination ($R^2 = 0.52, p < 0.01$) is identified between the average area of forest gained per patch size class in secondary forests, suggesting that gain is more pronounced in larger patches; however, this relationship is absent for patches harbouring primary forests ($R^2 = 0.14, p < 0.33$), with forest gain being uniformly absent across size classes (Figure 6C,D). This pattern is also reflected in Figure 5D, where larger patches experience on average greater loss areas than smaller fragments.

This pattern of greater than average losses in larger patches is potentially due to larger patches experiencing clear cutting more often, whereas smaller fragments—which are often nearer villages—experience a more selective logging [63]. Forest gain is greatest for larger forest patches, which may be the result of regrowth being possible in areas with lower anthropogenic impact, and in secondary regrowing forests [64,65].

3.2.2. Trends

To assess the temporal change dynamics of the forest fragments, average trends statistics were computed for forest patch size class. A significant positive coefficient of determination ($R^2 = 0.64, p < 0.01$) between forest patch size classes and Mann–Kendall trend is identified for secondary forest patches, suggesting generalized greening in larger secondary forest patches. In effect, such greening phenomenon has been widely reported by several authors and may be the result of shrub encroachment and land abandonment due to migration to the cities, and subsequently regrowth of shrubs, and overall lower human pressures [64,66–68]. This relationship is only weakly present in patches harbouring primary forest, suggesting regrowth or greening is not as pronounced.

3.2.3. Forest Change in Relation to Drivers

When examining forest loss and gain in relation to gHM, we find forest loss is larger for fragments in more modified landscapes of secondary forests ($R^2 = 0.32, p < 0.14$), and this is also the case for forest gain ($R^2 = 0.20, p < 0.3$). These results are probable as we expect more deforestation and regrowth to be occurring on modified landscapes. Further, we find that distance to roads and forest loss area are significantly positively related for secondary forests ($R^2 = 0.86, p < 0.001$) and to a lesser extent for primary forests ($R^2 = 0.32, p < 0.11$). Distance to roads and forest gain area are significantly negatively related to secondary forests ($R^2 = 0.53, p < 0.03$), and to a lesser extent to primary forests ($R^2 = 0.25, p < 0.17$). Thus, as distance to roads increases, forest loss increases, while the opposite is true for forest gain, namely, most gain occurs close to roads. These results may suggest that in general, regrowth after deforestation is occurring closer to roads, while deforestation continues further away from them.

3.2.4. Tree Cover and Height

Finally, we estimate how average tree cover and tree height vary across forest patch size classes, and so test the hypothesis that smaller patches have a lower cover and tree height, presumably as they are more heavily impacted by humans. A positive coefficient of determination is identified between mean tree cover (%) and forest patch size class ($R^2 = 0.56, p < 0.02$), with increasing patch size showing concurrent increases in mean tree cover. Similarly, mean tree height in meters and size classes exhibit a weak positive coefficient of determination ($R^2 = 0.29, p < 0.13$), with larger patches harbouring higher trees on average. These results suggest that larger forest patches may sustain denser tree cover and higher trees, potentially as results of being less impacted by human pressures.

4. Conclusions

This study mapped and inventoried for the first time West Africa forest patches based on multi-source satellite remote sensing and ancillary datasets and appraised their changes across size classes over the past 45 years. In doing so, it identified regional ecological change patterns useful to inform and facilitate conservation actions and sustainable use. The bulk of fragments identified are small, secondary forests; these experienced the most pronounced overall loss, with small forest patches undergoing cumulatively more forest loss compared

to larger patches—although considerable forest losses occur in large forest patches. Forest gain is comparatively negligible throughout the study area. Primary forest patches are scarcer and underwent fewer losses, presumably as they are less accessible. Moist forest, savanna and mangroves contribute importantly to the overall numbers of primary forest patches across size classes, highlighting the conservation importance of these biomes. In 1975 most patches were mapped as secondary forest land covers, particularly degraded forests, savanna, woodland, and mangrove; relatively few comprised human land-uses, such as cropland, settlements, and agriculture, suggesting that new forest patches do not often emerge/transition from arable land (at least over the past 45 years), but rather are remnants of previously forested landscapes such as savanna, woodland, and mangrove. We find widespread greening of larger fragments in secondary forests, a phenomenon observed in numerous studies and possibly the result of shrub encroachment and regrowth due to cropland abandonment, as well as lower human pressures due to emigration to urban centres. Forest loss and gain are more important across fragments lying in more modified landscapes of secondary forests; in contrast, as distance to roads increases, forest loss increases, while the forest gain is larger closer to roads, on average. Finally, larger forest patches were found to harbour a denser tree cover and higher trees on average, potentially as a result of being less impacted by human pressures.

Analyses in this study were limited by a lack of historical landscape data and dependence on medium-scale (Landsat) resolution data. In particular, historical satellite imagery spanning the decades before the year 2000 could have helped identify the age of forests more clearly. In addition, plantations could not be differentiated from the forest fragments—such an effort would have required more time resources than was available for this study and therefore is upcoming work. In conclusion, this inventory and change appraisal of small forest patches outside protected areas and embedded in agricultural landscapes forms the basis for understanding forest patch change and status, prioritizing them for in-depth, social-ecological field investigations, and helping to focus strategies for their conservation and sustainable use. Potential research drawing on this inventory, would be for example, to identify and analyse forest patch typologies, develop indices for biodiversity assessments, conduct in-depth analysis of the multifunctionality and ecosystem services of selected forest patches, or to identify which governance arrangements or social-ecological factor constellations foster forest persistence, resurgence, or the emergence/creation of new forests. Importantly, West African tropical forests are expected to further decline, with a concurrent increase of forest fragmentation and accompanying edge effect. Lacking any conservation status, diminishing in area, and subject to increasing extractive demands, understanding how to conserve and manage them sustainably for the benefit of an increasing population is imperative.

Author Contributions: V.R.W., conception, methodology design, analysis, and writing; C.I.S., funding acquisition, conception, methodology design, writing, edits, and supervision; F.O.A., conception, methodology design and edits; C.J.I. methodology design and edits. All authors have read and agreed to the published version of the manuscript.

Funding: This project has received funding from the European Research Council (ERC) under the European Union’s Horizon 2020 research and innovation programme (grant agreement No 101001200—SUSTAINFORESTS).

Data Availability Statement: The data are available upon request from the corresponding author.

Acknowledgments: We are grateful for free access to the datasets used and would like to thank anonymous reviewers for their valuable comments on the manuscript. This study contributes to the Programme on Ecosystem Change and Society (<https://pecs-science.org/>) and the Global Land Programme (<https://www.glp.earth/>).

Conflicts of Interest: The authors declare no conflict of interest.

References

- Barlow, J.; Gardner, T.A.; Araujo, I.S.; Ávila-Pires, T.C.; Bonaldo, A.B.; Costa, J.E.; Esposito, M.C.; Ferreira, L.V.; Hawes, J.; Hernandez, M.I.M.; et al. Quantifying the Biodiversity Value of Tropical Primary, Secondary, and Plantation Forests. *Proc. Natl. Acad. Sci. USA* **2007**, *104*, 18555–18560. [[CrossRef](#)] [[PubMed](#)]
- Gibson, L.; Lee, T.M.; Koh, L.P.; Brook, B.; Gardner, T.A.; Barlow, J.; Peres, C.; Bradshaw, C.; Laurance, W.F.; Lovejoy, T.E.; et al. Primary forests are irreplaceable for sustaining tropical biodiversity. *Nature* **2011**, *478*, 378–381. [[CrossRef](#)] [[PubMed](#)]
- Achard, F.; Beuchle, R.; Mayaux, P.; Stibig, H.; Bodart, C.; Brink, A.; Carboni, S.; Desclée, B.; Donnay, F.; Eva, H.D.; et al. Determination of Tropical Deforestation Rates and Related Carbon Losses from 1990 to 2010. *Glob. Chang. Biol.* **2014**, *20*, 2540–2554. [[CrossRef](#)] [[PubMed](#)]
- Mitchard, E.T. The tropical forest carbon cycle and climate change. *Nature* **2018**, *559*, 527–534. [[CrossRef](#)]
- Haddad, N.M.; Brudvig, L.A.; Clobert, J.; Davies, K.F.; Gonzalez, A.; Holt, R.D.; Lovejoy, T.E.; Sexton, J.O.; Austin, M.P.; Collins, C.D.; et al. Habitat Fragmentation and Its Lasting Impact on Earth’s Ecosystems. *Sci. Adv.* **2015**, *1*, e1500052. [[CrossRef](#)] [[PubMed](#)]
- Brinck, K.; Fischer, R.; Groeneveld, J.; Lehmann, S.; De Paula, M.D.; Pütz, S.; Sexton, J.O.; Song, D.; Huth, A. High resolution analysis of tropical forest fragmentation and its impact on the global carbon cycle. *Nat. Commun.* **2017**, *8*, 14855. [[CrossRef](#)] [[PubMed](#)]
- Chaplin-Kramer, R.; Ramler, I.; Sharp, R.R.; Haddad, N.M.; Gerber, J.; West, P.C.; Mandle, L.; Engstrom, P.; Baccini, A.; Sim, S.; et al. Degradation in carbon stocks near tropical forest edges. *Nat. Commun.* **2015**, *6*, 10158. [[CrossRef](#)] [[PubMed](#)]
- Laurance, W.F.; Camargo, J.L.; Luizão, R.C.; Laurance, S.G.; Pimm, S.L.; Bruna, E.M.; Stouffer, P.C.; Williamson, G.B.; Benítez-Malvido, J.; Vasconcelos, H.L.; et al. The fate of Amazonian forest fragments: A 32-year investigation. *Biol. Conserv.* **2011**, *144*, 56–67. [[CrossRef](#)]
- Pütz, S.; Groeneveld, J.; Henle, K.; Knogge, C.; Martensen, A.C.; Metz, M.; Metzger, J.P.; Ribeiro, M.C.; de Paula, M.D.; Huth, A. Long-term carbon loss in fragmented Neotropical forests. *Nat. Commun.* **2014**, *5*, 5037. [[CrossRef](#)]
- Qie, L.; Lewis, S.L.; Sullivan, M.J.P.; Lopez-Gonzalez, G.; Pickavance, G.C.; Sunderland, T.; Ashton, P.; Hubau, W.; Abu Salim, K.; Aiba, S.-I.; et al. Long-term carbon sink in Borneo’s forests halted by drought and vulnerable to edge effects. *Nat. Commun.* **2017**, *8*, 1966. [[CrossRef](#)]
- Seymour, F.; Harris, N.L. Reducing tropical deforestation. *Science* **2019**, *365*, 756–757. [[CrossRef](#)] [[PubMed](#)]
- Curtis, P.G.; Slay, C.M.; Harris, N.L.; Tyukavina, A.; Hansen, M.C. Classifying drivers of global forest loss. *Science* **2018**, *361*, 1108–1111. [[CrossRef](#)] [[PubMed](#)]
- Akinyemi, F.O.; Speranza, C.I. Agricultural Landscape Change Impact on the Quality of Land: An African Continent-Wide Assessment in Gained and Displaced Agricultural Lands. *Int. J. Appl. Earth Obs. Geoinf.* **2022**, *106*, 102644. [[CrossRef](#)]
- Groeneveld, J.; Alves, L.; Bernacci, L.; Catharino, E.; Knogge, C.; Metzger, J.; Pütz, S.; Huth, A. The impact of fragmentation and density regulation on forest succession in the Atlantic rain forest. *Ecol. Model.* **2009**, *220*, 2450–2459. [[CrossRef](#)]
- Ordway, E.M.; Asner, G.P. Carbon declines along tropical forest edges correspond to heterogeneous effects on canopy structure and function. *Proc. Natl. Acad. Sci. USA* **2020**, *117*, 7863–7870. [[CrossRef](#)]
- Broadbent, E.N.; Asner, G.P.; Keller, M.; Knapp, D.E.; Oliveira, P.J.; Silva, J.N. Forest fragmentation and edge effects from deforestation and selective logging in the Brazilian Amazon. *Biol. Conserv.* **2008**, *141*, 1745–1757. [[CrossRef](#)]
- Gascon, C.; Williamson, G.B.; da Fonseca, G.A.B. Receding Forest Edges and Vanishing Reserves. *Science* **2000**, *288*, 1356–1358. [[CrossRef](#)] [[PubMed](#)]
- Fischer, R.; Taubert, F.; Müller, M.S.; Groeneveld, J.; Lehmann, S.; Wiegand, T.; Huth, A. Accelerated forest fragmentation leads to critical increase in tropical forest edge area. *Sci. Adv.* **2021**, *7*, eabg7012. [[CrossRef](#)]
- Hansen, M.C.; Potapov, P.V.; Moore, R.; Hancher, M.; Turubanova, S.A.; Tyukavina, A.; Thau, D.; Stehman, S.V.; Goetz, S.J.; Loveland, T.R.; et al. High-resolution global maps of 21st-century forest cover change. *Science* **2013**, *342*, 850–853. [[CrossRef](#)]
- Hansen, M.C.; Wang, L.; Song, X.-P.; Tyukavina, A.; Turubanova, S.; Potapov, P.V.; Stehman, S.V. The fate of tropical forest fragments. *Sci. Adv.* **2020**, *6*, eaax8574. [[CrossRef](#)]
- Hecht, S.B.; Saatchi, S.S. Globalization and Forest Resurgence: Changes in Forest Cover in El Salvador. *BioScience* **2007**, *57*, 663–672. [[CrossRef](#)]
- Fairhead, J.; Leach, M. *Misreading the African Landscape: Society and Ecology in a Forest-Savanna Mosaic*; Cambridge University Press: Cambridge, UK, 1996; ISBN 0-521-56499-9.
- Lewis, S.L.; Lopez-Gonzalez, G.; Sonké, B.; Affum-Baffoe, K.; Baker, T.R.; Ojo, L.O.; Phillips, O.L.; Reitsma, J.M.; White, L.; Comiskey, J.A.; et al. Increasing Carbon Storage in Intact African Tropical Forests. *Nature* **2009**, *457*, 1003–1006. [[CrossRef](#)] [[PubMed](#)]
- Parnell, S.; Walawege, R. Sub-Saharan African urbanisation and global environmental change. *Glob. Environ. Chang.* **2011**, *21*, S12–S20. [[CrossRef](#)]
- Malhi, Y.; Hamilton, S.E.; Hill, S.L.L.; Arnell, A.; Maney, C.; Butchart, S.H.M.; Hilton-Taylor, C.; Ciciarelli, C.; Davis, C.; Dinerstein, E.; et al. Measuring Forest Biodiversity Status and Changes Globally. *Front. For. Glob. Chang.* **2019**, *1*, 70. [[CrossRef](#)]
- German, L.; Schoneveld, G.; Mwangi, E. Contemporary Processes of Large-Scale Land Acquisition in Sub-Saharan Africa: Legal Deficiency or Elite Capture of the Rule of Law? *World Dev.* **2013**, *48*, 1–18. [[CrossRef](#)]
- Allen, T.; Heinrig, P.; Heo, I. Agriculture, Food and Jobs in West Africa. *West African Papers*, 5 April 2018.

28. Cotillon, S.E.; Tappan, G.G. *Landscapes of West Africa: A Window on a Changing World*; United States Geological Survey: Garretson, SD, USA, 2016.
29. Nicholson, S.E. The West African Sahel: A Review of Recent Studies on the Rainfall Regime and Its Interannual Variability. *Int. Sch. Res. Not.* **2013**, *2013*, 453521. [[CrossRef](#)]
30. Keay, R. Derived Savanna: Derived from What. *Bull. l'Ifan* **1959**, *21*, 427–438.
31. Valentin, C. *Rapport Sur La Résidence Du Kissi*; National Archives: Dakar, Senegal, 1893.
32. Adam, J. Les Reliques Boisées et Les Essences Des Savanes Dans La Zone Préforestière En Guinée Française. *Bull. Soc. Bot. Fr.* **1948**, *95*, 22–26. [[CrossRef](#)]
33. Gouvernement de Guinée, C. *Politique Forestière et Plan d'action, Plan d'Action Forestier Tropical*, 1988; Food and Agriculture Organization of the United Nations: Rome, Italy, 1988.
34. Aubréville, A. Climats, Forêts et Désertification de l'Afrique Tropicale. 1949. Available online: <https://agris.fao.org/agris-search/search.do?recordID=US201300651842> (accessed on 27 September 2022).
35. Keay, R.W.J. *Vegetation Map of Africa South of the Tropic of Cancer. Explanatory Notes*; Oxford University Press: Oxford, UK, 1959.
36. Gayibor, N.L. *Écologie et Histoire: Les Origines de La Savane Du Bénin (Ecology and History: The Origins of the Benin Savanna)*. *Cah. D'études Afr.* **1986**, *26*, 13–41.
37. Backéus, I. Distribution and vegetation dynamics of humid savannas in Africa and Asia. *J. Veg. Sci.* **1992**, *3*, 345–356. [[CrossRef](#)]
38. Sinsin, B.; Kampmann, D.; Thiombiano, A.; Konaté, S. Atlas de La Biodiversité de l'Afrique de l'Ouest, Tome III: Côte d'Ivoire. Abidjan & Frankfurt/Main. 2010. Available online: http://www.goethe-university-frankfurt.de/50800968/CI_01_Cover_Preface_Introduction.pdf (accessed on 27 September 2022).
39. Gorelick, N.; Hancher, M.; Dixon, M.; Ilyushchenko, S.; Thau, D.; Moore, R. Google Earth Engine: Planetary-scale geospatial analysis for everyone. *Remote Sens. Environ.* **2017**, *202*, 18–27. [[CrossRef](#)]
40. Keenan, R.J.; Reams, G.A.; Achard, F.; de Freitas, J.V.; Grainger, A.; Lindquist, E. Dynamics of Global Forest Area: Results from the FAO Global Forest Resources Assessment 2015. *For. Ecol. Manag.* **2015**, *352*, 9–20. [[CrossRef](#)]
41. Potapov, P.; Li, X.; Hernandez-Serna, A.; Tyukavina, A.; Hansen, M.C.; Kommareddy, A.; Pickens, A.; Turubanova, S.; Tang, H.; Silva, C.E.; et al. Mapping global forest canopy height through integration of GEDI and Landsat data. *Remote Sens. Environ.* **2021**, *253*, 112165. [[CrossRef](#)]
42. UNEP-WCMC; IUCN. *NGS (2018) Protected Planet Report 2018*; UNEP-WCMC: Cambridge, UK; IUCN: Gland, Switzerland; NGS: Washington, DC, USA, 2020.
43. Maxwell, S.L.; Evans, T.; Watson, J.E.M.; Morel, A.; Grantham, H.; Duncan, A.; Harris, N.; Potapov, P.; Runting, R.K.; Venter, O.; et al. Degradation and forgone removals increase the carbon impact of intact forest loss by 626%. *Sci. Adv.* **2019**, *5*, eaax2546. [[CrossRef](#)] [[PubMed](#)]
44. Turubanova, S.; Potapov, P.V.; Tyukavina, A.; Hansen, M.C. Ongoing Primary Forest Loss in Brazil, Democratic Republic of the Congo, and Indonesia. *Environ. Res. Lett.* **2018**, *13*, 074028. [[CrossRef](#)]
45. Dinerstein, E.; Olson, D.; Joshi, A.; Vynne, C.; Burgess, N.D.; Wikramanayake, E.; Hahn, N.; Palminteri, S.; Hedao, P.; Noss, R.; et al. An Ecoregion-Based Approach to Protecting Half the Terrestrial Realm. *Bioscience* **2017**, *67*, 534–545. [[CrossRef](#)]
46. Food and Agriculture Organization of the United Nations. *The Global Administrative Unit Layers (GAUL): Technical Aspects*; Food and Agriculture Organization of the United Nations: Rome, Italy, 2008.
47. Solórzano, J.V.; Gallardo-Cruz, J.A.; Peralta-Carreta, C.; Martínez-Camilo, R.; de Oca, A.F.-M. Plant community composition patterns in relation to microtopography and distance to water bodies in a tropical forested wetland. *Aquat. Bot.* **2020**, *167*, 103295. [[CrossRef](#)]
48. Pekel, J.-F.; Cottam, A.; Gorelick, N.; Belward, A.S. High-resolution mapping of global surface water and its long-term changes. *Nature* **2016**, *540*, 418–422. [[CrossRef](#)]
49. Center for International Earth Science Information Network-CIESIN-Columbia University and Information Technology Outreach Services-ITOS-University of Georgia. *Global Roads Open Access Data Set, Version 1 (GROADSv1)*; NASA Socioeconomic Data and Applications Center (SEDAC): Palisades, NY, USA, 2013. [[CrossRef](#)]
50. Kennedy, C.M.; Oakleaf, J.R.; Theobald, D.M.; Baruch-Mordo, S.; Kiesecker, J. Managing the middle: A shift in conservation priorities based on the global human modification gradient. *Glob. Chang. Biol.* **2019**, *25*, 811–826. [[CrossRef](#)]
51. Kennedy, C.; Oakleaf, J.R.; Theobald, D.M.; Baruch-Mordo, S.; Kiesecker, J. *Documentation for the Global Human Modification of Terrestrial Systems*; NASA Socioeconomic Data and Applications Center (SEDAC): Palisades, NY, USA, 2020.
52. Myers-Smith, I.H.; Kerby, J.T.; Phoenix, G.K.; Bjerke, J.W.; Epstein, H.E.; Assmann, J.J.; John, C.; Andreu-Hayles, L.; Angers-Blondin, S.; Beck, P.S.A.; et al. Complexity revealed in the greening of the Arctic. *Nat. Clim. Chang.* **2020**, *10*, 106–117. [[CrossRef](#)]
53. Forkel, M.; Carvalhais, N.; Verbesselt, J.; Mahecha, M.D.; Neigh, C.S.R.; Reichstein, M. Trend Change Detection in NDVI Time Series: Effects of Inter-Annual Variability and Methodology. *Remote Sens.* **2013**, *5*, 2113–2144. [[CrossRef](#)]
54. Verbesselt, J.; Hyndman, R.; Newnham, G.; Culvenor, D. Detecting trend and seasonal changes in satellite image time series. *Remote Sens. Environ.* **2010**, *114*, 106–115. [[CrossRef](#)]
55. Pohlert, T. Non-Parametric Trend Tests and Change-Point Detection. 2016. Available online: <https://cran.microsoft.com/snapshot/2017-11-08/web/packages/trend/vignettes/trend.pdf> (accessed on 1 March 2021).
56. Theil, H. A Rank-Invariant Method of Linear and Polynomial Regression Analysis. *Indag. Math.* **1950**, *12*, 173.

57. Morell, O.; Fried, R. On Nonparametric Tests for Trend Detection in Seasonal Time Series. In *Statistical Inference, Econometric Analysis and Matrix Algebra*; Springer: Berlin/Heidelberg, Germany, 2009; pp. 19–39.
58. Congalton, R.G.; Green, K. *Assessing the Accuracy of Remotely Sensed Data: Principles and Practices*; CRC Press: Boca Raton, FL, USA, 2019; ISBN 0-429-62935-4.
59. Planet Team. *Planet Application Program Interface: In Space for Life on Earth*; Planet Team: San Francisco, CA, USA, 2017; Volume 2017, p. 40.
60. Potapov, P.; Hansen, M.C.; Laestadius, L.; Turubanova, S.; Yaroshenko, A.; Thies, C.; Smith, W.; Zhuravleva, I.; Komarova, A.; Minnemeyer, S. The Last Frontiers of Wilderness: Tracking Loss of Intact Forest Landscapes from 2000 to 2013. *Sci. Adv.* **2017**, *3*, e1600821. [[CrossRef](#)]
61. Bryan-Brown, D.N.; Connolly, R.M.; Richards, D.R.; Adame, F.; Friess, D.A.; Brown, C.J. Global trends in mangrove forest fragmentation. *Sci. Rep.* **2020**, *10*, 7177. [[CrossRef](#)] [[PubMed](#)]
62. Poorter, L.; Craven, D.; Jakovac, C.C.; van der Sande, M.T.; Amissah, L.; Bongers, F.; Chazdon, R.L.; Farrior, C.E.; Kambach, S.; Meave, J.A.; et al. Multidimensional tropical forest recovery. *Science* **2021**, *374*, 1370–1376. [[CrossRef](#)] [[PubMed](#)]
63. Neuenschwander, P.; Bown, D.; Hédégbètan, G.C.; Adomou, A. Long-Term Conservation and Rehabilitation of Threatened Rain Forest Patches under Different Human Population Pressures in West Africa. *Nat. Conserv.* **2015**, *13*, 21–46. [[CrossRef](#)]
64. Mitchard, E.T.A.; Saatchi, S.S.; Lewis, S.L.; Feldpausch, T.R.; Woodhouse, I.H.; Sonké, B.; Rowland, C.; Meir, P. Measuring biomass changes due to woody encroachment and deforestation/degradation in a forest–savanna boundary region of central Africa using multi-temporal L-band radar backscatter. *Remote Sens. Environ.* **2011**, *115*, 2861–2873. [[CrossRef](#)]
65. Wingate, V.R.; Phinn, S.R.; Kuhn, N.; Scarth, P. Estimating aboveground woody biomass change in Kalahari woodland: Combining field, radar, and optical data sets. *Int. J. Remote Sens.* **2018**, *39*, 577–606. [[CrossRef](#)]
66. Venter, Z.; Cramer, M.D.; Hawkins, H.-J. Drivers of woody plant encroachment over Africa. *Nat. Commun.* **2018**, *9*, 2272. [[CrossRef](#)]
67. Olsson, L.; Eklundh, L.; Ardö, J. A recent greening of the Sahel—Trends, patterns and potential causes. *J. Arid. Environ.* **2005**, *63*, 556–566. [[CrossRef](#)]
68. de Jong, R.; Verbesselt, J.; Zeileis, A.; Schaepman, M.E. Shifts in Global Vegetation Activity Trends. *Remote Sens.* **2013**, *5*, 1117–1133. [[CrossRef](#)]